

# *a/c* YBa<sub>2</sub>Cu<sub>3</sub>O<sub>7</sub> boundaries: Preferential sites for the nucleation of epitaxial Y<sub>2</sub>O<sub>3</sub> precipitates

A. Catana, D. G. Schlom, J. Mannhart, and J. G. Bednorz

IBM Research Division, Zurich Research Laboratory, 8803 Rüschlikon, Switzerland

(Received 12 March 1992; accepted for publication 26 May 1992)

Y<sub>2</sub>O<sub>3</sub> precipitates with typical sizes between 70 and 300 nm<sup>2</sup> have been identified by high-resolution electron microscopy and image calculations in mixed *a*- and *c*-axis oriented YBa<sub>2</sub>Cu<sub>3</sub>O<sub>7</sub> sputtered films. The precipitates are densely distributed (10<sup>15</sup> cm<sup>-3</sup>), have tabular shape and grow epitaxially at boundaries between *a*- and *c*-axis oriented grains, with the (001) Y<sub>2</sub>O<sub>3</sub> plane parallel to the *a,b* plane of the *a*-axis oriented grain and the (110) Y<sub>2</sub>O<sub>3</sub> plane parallel to the *a,b* plane of the *c*-axis oriented grain. Their largest interfacial facet lies parallel to the *a,b* plane of the *a*-axis oriented regions. Lattice-matching arguments show that energetically this situation is the most favorable one, which explains the nucleation of precipitates at *a/c* boundaries.

The understanding of the microstructure of high *T<sub>c</sub>* films is not only essential for applications, but should also provide valuable insights into the growth mechanisms. Defects play an essential role in controlling the growth process, the superconducting and non-superconducting properties of such films. This motivates the study of the structure and morphology of impurity phases, their formation and their impact on the resulting structure of slightly nonstoichiometric films. Concerning the surfaces of such films, it has been shown that they are strongly dependent on composition.<sup>1,2</sup> However, off-stoichiometry also results in features embedded inside the films, such as line and point defects, stacking faults and precipitates. To investigate how stoichiometry and processing parameters influence the distribution of second phases and other features embedded inside the films, a detailed structural characterization is required.

A number of studies have focused on the characterization of second phases that are incorporated in YBCO films which were grown by various techniques. In particular, it has been reported that in sputtered and laser-ablated films, YBa<sub>2</sub>Cu<sub>2</sub>O<sub>7</sub> precipitates are present at boundaries between *a*- and *c*-axis YBCO domains where it was suggested that they act as nucleation sites for *a,b* domains.<sup>3</sup> Other groups have reported on other impurity phases: Y<sub>2</sub>O<sub>3</sub>, CuO, Y<sub>2</sub>Cu<sub>2</sub>O<sub>5</sub>, and Y<sub>2</sub>BaCuO<sub>5</sub> in laser-ablated films,<sup>4</sup> Y<sub>2</sub>O<sub>3</sub> in sputtered films,<sup>5</sup> and CuYO<sub>2</sub> in films prepared by electron beam coevaporation.<sup>6,7</sup>

Y<sub>2</sub>O<sub>3</sub> is cubic (*a*=1.06 nm) and belongs to the space *Ia*3. The dominant orientation of Y<sub>2</sub>O<sub>3</sub> particles with respect to pure *c*-axis oriented films was determined to be [100]Y<sub>2</sub>O<sub>3</sub> || [110]YBCO, (001) Y<sub>2</sub>O<sub>3</sub> || (001) YBCO.<sup>5</sup> It has been shown that this orientation relationship also describes Y<sub>2</sub>O<sub>3</sub> buffer layers grown on *c*-axis oriented YBCO.<sup>8,9</sup>

This letter focuses on Y<sub>2</sub>O<sub>3</sub> inclusions in mixed *a*- and *c*-axis oriented YBa<sub>2</sub>Cu<sub>3</sub>O<sub>7</sub> (YBCO) films, thereby presenting complementary results to those for *c*-axis films.<sup>5</sup> We report on the structure of the precipitates and on their epitaxial orientations with respect to YBCO, as obtained from electron diffraction, high-resolution electron micros-

copy (HREM) and image calculations. In addition, the present relevance of second phases for the growth of domains having their *a* or *b* axis normal to the substrate surface (*a*-axis domains)<sup>3</sup> is investigated.

The YBCO films were grown by dc hollow cathode magnetron sputtering<sup>10</sup> on SrTiO<sub>3</sub> (001) and Sr<sub>2</sub>RuO<sub>4</sub> (001)<sup>11</sup> substrates at substrate heater block temperatures (*T<sub>sub</sub>*) ranging from 650 to 750 °C. The sputtering pressure was 650 mTorr (Ar/O<sub>2</sub>=2:1), the plasma discharge was operated at 450 mA and 150–170 V, and after growth, the films were cooled at room temperature within 1 h in 0.15 bar O<sub>2</sub>.

Transmission electron microscopy samples were prepared for both planar and cross-sectional views by standard mechanical polishing and ion milling with liquid nitrogen cooling. The observations were performed on a JEOL JEM-2010 operating at 200 kV. Image calculations were performed using the EMS software package developed by Stadelmann.<sup>12</sup>

Figure 1(a) shows low-magnification HREM image of a mixed *a*- and *c*-axis oriented YBCO film; about 50% of the film is a *a*-axis oriented. Precipitates with sizes between 70 and 300 nm<sup>2</sup> and density of the order of 10<sup>15</sup> cm<sup>-3</sup> are observed at both *a/c* and *a/a* (90° in-plane rotation twins) boundaries. The precipitates predominantly exhibit tabular habit; they are elongated along the *a,b* plane of the *a*-axis regions [Fig. 1(b)]. At *a/a* boundaries the thickness/width ratio and the precipitate size (up to 600 nm<sup>2</sup>) increase. The corresponding electron diffraction pattern [Fig. 1(c)] is consistent with the precipitates being Y<sub>2</sub>O<sub>3</sub>. Their dominant epitaxial relationship with respect to the *c*-axis oriented regions is [110] Y<sub>2</sub>O<sub>3</sub> || [001] YBCO, (001) Y<sub>2</sub>O<sub>3</sub> || (100) YBCO, which is different from the orientation of those particles that are fully embedded in regions of this type.<sup>5</sup>

The nucleation of the precipitates can be explained on the basis of lattice-matching arguments. The *a,b* plane of YBCO has the smallest lattice mismatch to (001) Y<sub>2</sub>O<sub>3</sub>: 3% along [110] Y<sub>2</sub>O<sub>3</sub> || [100] YBCO, with a nearly coincident unit cell area of 1.1 nm<sup>2</sup> [Fig. 2(a)] The lattice match of the (110) Y<sub>2</sub>O<sub>3</sub> plane to the *a,b* plane of YBCO is not as

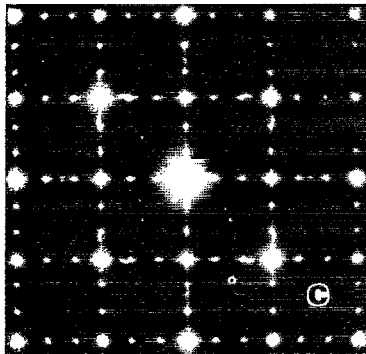
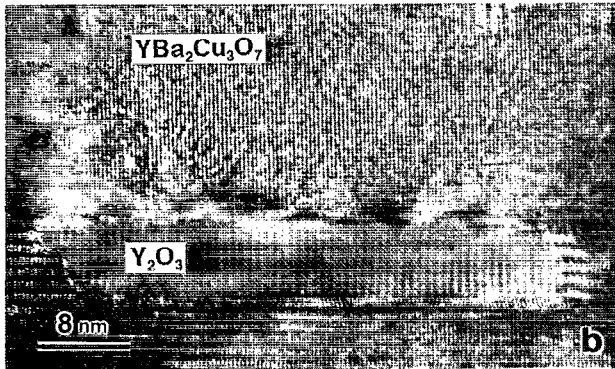
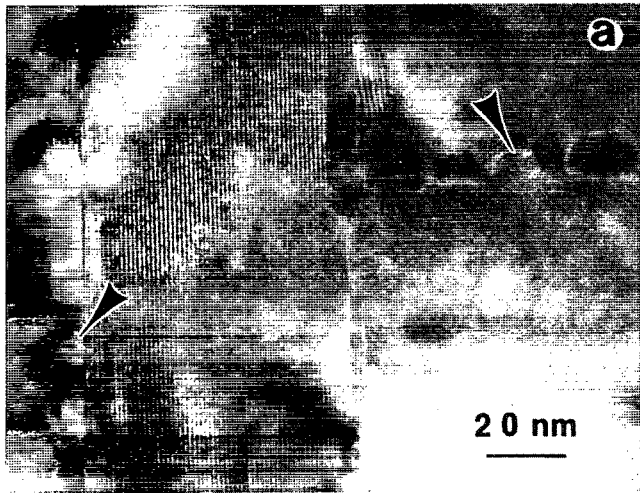


FIG. 1. (a) Planar-view micrograph of mixed  $a$  and  $c$  YBCO domains and second-phase inclusions (arrows). (b) HREM image of a  $Y_2O_3$  precipitate with tabular shape at an  $a/c$  boundary. (c) Electron diffraction pattern along the substrate normal;  $Y_2O_3$  100- and 110-type reflections overlap with YBCO 100-type spots.

favorable: 9% along  $[001] Y_2O_3 \parallel [010] YBCO$  and 3% along  $[110] Y_2O_3 \parallel [100] YBCO$ , with a nearly coincident unit cell area of  $1.7 \text{ nm}^2$  [Fig. 2(b)]. Hence, joining  $(110) Y_2O_3$  to the  $a, b$  plane of YBCO requires larger nearly coincident cells and deformations and is thus energetically less favorable than joining  $(001) Y_2O_3$  to the  $a, b$  plane. The high density of atomic coincidences in this latter plane as well as minimal strain promote growth, which in turn leads to the formation of larger interfacial areas and to the observed precipitate elongation.

It is interesting to note that precipitates have not been observed to grow inside  $a$ -axis domains. This is partly due to the poor matching between  $[001] Y_2O_3$  and  $[001] YBCO$

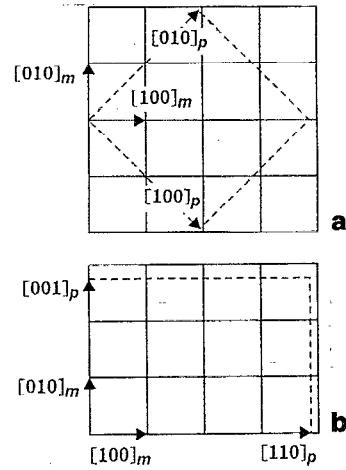


FIG. 2. Superimposed lattice points indicating nearly coincident unit cells in the interfacial planes: (a)  $(001) Y_2O_3 \parallel (001) YBCO$  and (b)  $(110) Y_2O_3 \parallel (001) YBCO$ . At  $a/c$  boundaries the precipitates have interface of type (a) along the  $a$ -axis grain and of type (b) along the  $c$ -axis grain. Solid lines and  $m$  (matrix) subscripts indicate YBCO, dashed lines and  $p$  (precipitate) subscripts  $Y_2O_3$ .

(10%). However, lattice matching arguments alone cannot explain this feature since such precipitates have been observed to nucleate inside  $c$ -axis films deposited at higher temperatures.<sup>5</sup> Other features such as the growth kinetics of the  $a$ -axis oriented grains ought to be considered to explain the growth of these second phases. Particularly, the large number of domain boundaries present in mixed  $a$ - and  $c$ -oriented films, providing favorable sites for the segregation of second phases, seems to be relevant.

For an unambiguous identification of these precipitates, we compared HREM micrographs to calculated images. The  $[110]$  projection of the  $Y_2O_3$  unit cell is displayed in Fig. 3(a). Figure 3(b) shows a HREM micrograph of  $Y_2O_3$  and, superimposed, the matching calculated image obtained with the Bloch wave algorithm of the EMS software package.<sup>12</sup> The sample thickness was estimated to be 6 nm, while the focusing conditions ( $66 \text{ nm}^{-1}$ ) were determined on the basis of diffractograms. For the calculation parameters used, the image favorably matches the experimental micrograph: it clearly shows the projection of the face-centered substructure of the Y atoms (bright dots) for which the  $(111)$  planes cross at an angle of  $70.5^\circ$ .

In addition to the observation of epitaxial  $Y_2O_3$  pre-

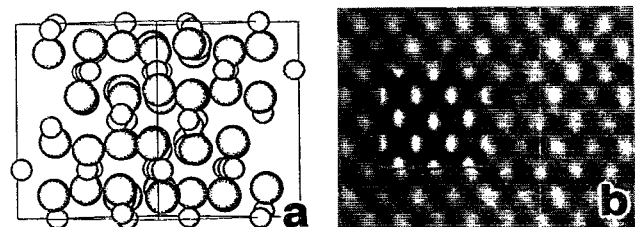


FIG. 3. (a)  $[110]$  projection of the  $Y_2O_3$  structure (small circles represent metal atoms). (b) HREM micrograph of  $(110) Y_2O_3$  and matching calculated image (inset). The microscope parameters are: spherical aberration coefficient = 0.5 mm, spread of focus = 8 nm, beam semiconvergence = 0.8 mrad, defocus = 66 nm; sample thickness = 6 nm.

precipitates in films produced by laser ablation<sup>4</sup> and sputtering, there is also evidence of such precipitates in films grown by *e*-beam evaporation.<sup>6,7</sup> Although these impurities were not explicitly identified as Y<sub>2</sub>O<sub>3</sub> in this case, regions in the HREM micrographs closely match the calculated image [Fig. 3(b)]. Unassigned x-ray peaks<sup>7</sup> also corroborate the presence of Y<sub>2</sub>O<sub>3</sub>. On the basis of these results, we suggest that in addition to CuYO<sub>2</sub> also the occurrence of Y<sub>2</sub>O<sub>3</sub> should be considered in films by electron-beam co-evaporation. That Y<sub>2</sub>O<sub>3</sub> forms and persists in contact with YBCO is unexpected from the equilibrium phase diagram, which indicates that even at low oxygen pressures the two phases should react to produce Y<sub>2</sub>BaCuO<sub>5</sub> and either CuO, Cu<sub>2</sub>O, or BaCu<sub>2</sub>O<sub>2</sub>, depending on the oxygen pressure.<sup>13</sup> The existence of Y<sub>2</sub>O<sub>3</sub>/YBCO interfaces in films may be due to the kinetic hindrance of the nucleation and growth of the expected phases (mainly Y<sub>2</sub>CuO<sub>5</sub>) or to lower interfacial energies between YBCO and Y<sub>2</sub>O<sub>3</sub> than between YBCO and Y<sub>2</sub>BaCuO<sub>3</sub>. Considering the lattice-matching considerations presented and the highly oriented growth observed, this latter explanation appears more likely.

In summary, Y<sub>2</sub>O<sub>3</sub> precipitates in sputtered mixed *a*- and *c*-axis oriented YBCO films on SrTiO<sub>3</sub> substrates have been identified by HREM and image calculations. They exhibit tabular shape and grow epitaxially at *a/c* as well as at *a/a* boundaries. The orientation relationship with respect to the *c*-axis regions is [110] Y<sub>2</sub>O<sub>3</sub> || [001] YBCO, (001) Y<sub>2</sub>O<sub>3</sub> || (100) YBCO. Their largest interfacial facet lies parallel to the *a, b* plane of the *a*-axis regions, in agreement with predictions based on lattice-matching arguments. Although these results present additional evidence for the presence of second phases at *a/c* boundaries, it is

not concluded at this point that such inclusions directly influence the nucleation of *a*-axis oriented domains. Specifically, the predominance of (001) Y<sub>2</sub>O<sub>3</sub> || (001) YBCO of *a*-axis oriented grains over *c*-axis oriented grains suggests that these precipitations nucleate on preexisting *a*-axis grains rather than causing their formation. In addition, the observation of Y<sub>2</sub>O<sub>3</sub> precipitates indicates that a straight line joins Y<sub>2</sub>O<sub>3</sub> to YBCO in the phase diagram that applies to our deposition conditions.

The authors gratefully acknowledge F. Lichtenberg for providing the Sr<sub>2</sub>RuO<sub>4</sub> substrates and R. F. Broom for his valuable support, as well as the financial support of the Swiss National Science Foundation.

- <sup>1</sup>J. A. Edwards, N. G. Chew, S. W. Goodyear, S. E. Blenkinsop, and R. G. Humphries, *J. Less-Common Metals* **164**, 414 (1990).
- <sup>2</sup>J. Zhao, C. S. Chern, Y. Q. Li, P. Norris, B. Gallois, B. Kear, X. D. Wu, and R. E. Münchhausen, *Appl. Phys. Lett.* **58**, 2839 (1991).
- <sup>3</sup>R. Ramesh, A. Inam, D. M. Hwang, T. D. Sands, C. C. Chang, and D. L. Hart, *Appl. Phys. Lett.* **58**, 1557 (1991).
- <sup>4</sup>O. Eibl and B. Roas, *J. Mater. Res.* **5**, 2620 (1990).
- <sup>5</sup>A. Catana, R. F. Broom, J. G. Bednorz, J. Mannhart, and D. G. Schlom, *Appl. Phys. Lett.* **60**, 1016 (1992).
- <sup>6</sup>A. F. Marshall, V. Matijasevic, P. Rosenthal, K. Shinohara, R. H. Hammond, and M. R. Beasley, *Appl. Phys. Lett.* **57**, 1158 (1990).
- <sup>7</sup>V. Matijasevic, P. Rosenthal, K. Shinohara, A. F. Marshall, R. H. Hammond, and M. R. Beasley, *J. Mater. Res.* **6**, 682 (1991).
- <sup>8</sup>K. Hirata, K. Yamaoto, K. Iijima, J. Takada, T. Terashima, Y. Bando, and H. Mazaki, *Appl. Phys. Lett.* **56**, 683 (1990).
- <sup>9</sup>Q. Y. Ying, C. Hilbert, N. Kumar, D. Eichman, M. Thompson, K. Kroger, and D. M. Hwang, *Appl. Phys. Lett.* **59**, 3036 (1991).
- <sup>10</sup>X. X. Xi, G. Linker, O. Meyer, E. Nold, B. Obst, F. Ratzel, R. Smithey, B. Strehlau, F. Weschenfelder, and J. Geerk, *Z. Phys. B* **74**, 13 (1989).
- <sup>11</sup>F. Lichtenberg, A. Catana, J. Mannhart, and D. G. Schlom, *Appl. Phys. Lett.* **60**, 1138 (1992).
- <sup>12</sup>P. Stadelmann, *Ultramicroscopy* **21**, 131 (1987).
- <sup>13</sup>R. Beyers and B. T. Ahn, *Annu. Rev. Mater. Sci.* **21**, 335 (1991).

Applied Physics Letters is copyrighted by AIP Publishing LLC (AIP). Reuse of AIP content is subject to the terms at: <http://scitation.aip.org/termsconditions>. For more information, see <http://publishing.aip.org/authors/rights-and-permissions>.